# Effect of electron spin-spin exchange interaction on spin precession in coupled quantum well



doi: 10.1063/1.3622324

# Effect of electron spin-spin exchange interaction on spin precession in coupled quantum well

Tetsu Ito,[1,2,a)] Wataru Shichi,[2] Masao Ichida,[2,3] Hideki Gotoh,[4] Hidehiko Kamada,[4] and Hiroaki Ando[2,3]

[1]*Division of Global Research Leaders, Shizuoka University, 3-5-1 Johoku, Naka-ku, Hamamatsu 432-8561, Japan*
[2]*Quantum Nano-Technology Laboratory, Konan University, 8-9-1 Okamoto, Higashinada-ku, Kobe 658-8501, Japan*
[3]*Graduate School of Natural Science, Konan University, 8-9-1 Okamoto, Higashinada-ku, Kobe 658-8501, Japan*
[4]*NTT Basic Research Laboratories, NTT Corporation, 3-1 Morinosato Wakamiya, Atsugi-shi, Kanagawa 243-0198, Japan*

(Received 3 March 2011; accepted 3 July 2011; published online 11 August 2011)

Electron spin-spin interaction in an asymmetric coupled quantum well (CQW) was investigated through electron spin-precession measurements. Precession (Larmor) frequencies from electrons localized in two CQWs were measured by means of polarization- and time-resolved photoluminescence measurements under a high magnetic field. At a low excitation power density, the Larmor frequency of the CQW was same as that of a single quantum well. The Larmor frequency of electron spin in one well was shifted to that in the other well as the excitation power density was increased. These experimental results are quantitatively explained by an exchange interaction between electrons localized in the two wells. © *2011 American Institute of Physics*. [doi:10.1063/1.3622324]

## I. INTRODUCTION

Recently, there has been a growing interest in electron-spin-related phenomena in semiconductor structures with respect to their scientific and technological potential. In fact, the utilization of spin degrees of freedom in semiconductors is paving the way toward quantum information technologies, including quantum computing, which assigns quantum bits (qubits) to the quantum states of localized electron spin,[1–6] and quantum media conversion from photon polarization qubits to electron spin qubits.[7,8] These studies on electron spin in semiconductors appear to be motivated by three lines of reasoning: First, the spin up-down states can be treated as a simple two-level system. Second, the spin coherence time is several orders of magnitude longer than that of an optical dipole in semiconductors. Third, the spin orientation is controllable and detectable with well-established optical methods. These possibilities make the electron spin attractive as a qubit.

When considering the application of the spin degree of freedom to qubits, the interaction between electron spins, that is, the spin-spin interaction, becomes a key factor. This is because the spin-spin interaction is indispensable to quantum logic gates.[2,3] On the other hand, the spin-spin interaction may destruct quantum states stored in spin memories. However, there have been few reports[9,10] on the electron spin-spin interaction in semiconductors, and the issue has yet to be investigated precisely. Physical understanding of the spin-spin interaction parameters, such as its energy and effective range is still insufficient for practical manipulation of q-bits in quantum computers. For applications in practical devices it is crucial to adequately elucidate the spin-spin interaction in semiconductor nanostructures. In order to evaluate spin-spin interaction, control of coupling between two spin systems must be achieved. When electron spins localized in quantum dots (QDs) are considered to be two spin systems for the spin-spin interaction measurements,[9] controlling the coupling between two QDs is not easy because of technological difficulty of position adjustment. In the study of intersubband excitonic interaction,[10] overlap of the first and second-subband exciton wave functions cannot be changed. Systematic evaluation of spin-spin interaction in quantum wells (QWs) is important for controlling the electron spin *g*-factor though the spin-spin interaction, which should be useful for spin-related application technologies such as quantum media conversion in QWs.[7,8]

The purpose of the present study is to clarify physics of the spin-spin interaction of two electron systems in asymmetric coupled quantum wells (CQWs), and thereby, reveal its physical origin. By changing the well width, separation, and barrier height in the CQW, its energy levels, overlap of the electronic wave functions, and *g*-factors of electron spins confined in two wells can be controlled.[11–14] This results in that energy separation, coupling strength between two electron systems, and spin precession frequency are able to be adjusted. Thus, it is effective to evaluate fundamental parameters related to the spin-spin interaction by investigating optical properties of CQW sample. In a series of experiments, the Larmor frequencies of the two electron systems were separately measured using time-resolved photoluminescence (PL) measurements[11–14] under a high magnetic field; the temporal changes in the optical polarization induced by the

a)Electronic mail: dtito@ipc.shizuoka.ac.jp.

 

spin precession were observed. A shift in the Larmor frequency was observed as the electron density was increased. Theoretical analyses considering the effective magnetic field caused by the spin-spin interaction were conducted on the basis of the density matrix method. Comparisons between experimental and theoretical analyses demonstrated that the spin-spin exchange interaction quantitatively accounts for the shift in the Larmor frequency of the electron spin.

## II. EXPERIMENTAL DETAILS

In the present study, we used a GaAs/AlGaAs coupled quantum well (CQW) and single quantum wells (SQWs) grown by molecular beam epitaxy (MBE). Structures of CQW and SQWs are schematically shown on the right-hand side of Fig. 1(a) and (b), respectively. In the CQW sample, each QW consists of an unintentionally doped ($<10^{16}$ cm$^{-3}$) GaAs well and $Al_{0.1}Ga_{0.9}As$ barrier layers grown on a (001) GaAs substrate. The thicknesses of the two well layers and the barrier layer between them are 10, 15, and 11 nm, respectively. For control experiments, we also investigated unintentionally doped ($<10^{16}$ cm$^{-3}$) GaAs/$Al_{0.1}Ga_{0.9}As$ SQWs with a well width of 10 or 15 nm grown on a (001) GaAs substrate. These SQWs are separated by an $Al_{0.1}Ga_{0.9}As$ barrier layer with a thickness of 50 nm. Polarization- and time-resolved PL measurements[11–14] were carried out to observe the electron-spin precession under a high magnetic field in Voigt configuration at 4 K. In the experiment, the QW samples were irradiated by a Ti-doped sapphire laser with a photon energy of 1.764 eV. The duration and repetition rate of the laser pulses were 2 ps and 80 MHz, respectively. The linearly polarized laser pulses were converted to circularly polarized pulses ($\sigma^+$ or $\sigma^-$) using a quarter-wave plate, after which the circularly polarized laser pulses illuminated the samples for selective excitation of spin-polarized electrons. The circularly polarized components in the PL signal emitted from the samples were selectively measured using a quarter-wave plate and a polarizer. The temporal changes in the intensity of the circular components were measured with a streak camera (Hamamatsu C5680).

Figure 1 shows PL spectra of (a) CQW and (b) SQWs measured with the streak camera in the absence of a magnetic field. The PL spectra are obtained by integrating the temporal change in the PL signal during 1.5 ns after photoexcitation. The emission peak around 1.515 eV is an emission from the GaAs buffer layer. The other two peaks in Fig. 1(a) are emissions of a higher (HC) and a lower (LC) mode of CQW. In the same manner, the two peaks in Fig. 1(b) are emissions from SQWs with a well width of 10 nm (HS) and 15 nm (LS). The emission photon energies of the HC and LC modes are almost the same as those of the HS and LS emissions, respectively. We designed the CQW structures such that the HC and LC modes are localized at the 10 and 15 nm QW. Therefore, the emission photon energy is observed at that of the corresponding well width. We also kept the barrier width sufficiently thin to observe the spin-spin interaction between the HC and LC modes. This condition caused a suppression of the PL intensity of the HC mode compared to the LC mode. However, the PL intensity of the HC mode is sufficiently strong for the spin-precession measurements. The PL spectra for the HC mode are observed as distinct peaks; the peak width of the LC mode under the highest excitation power (excitation density of $10^{11}$cm$^{-2}$) is almost the same as that under low excitation.

By increasing the magnetic field, we have observed an oscillation in the temporal evolution of the intensity difference between the circular components $\sigma^+$ and $\sigma^-$ reflecting the electron-spin precession as shown in Fig. 2. The excitation power density was varied from 48 to 890 W/cm$^2$. The oscillation frequency of HC mode seems to shift to that of LC mode with increasing the excitation power density. To clarify this frequency shift precisely, the time-domain signal was converted by Fourier transform (FT) to a frequency-domain signal. The excitation power dependence of the FT spectra under a magnetic field of 2 T for (a) the LC mode, (b) the HC mode, and (c) the HS emission are shown in

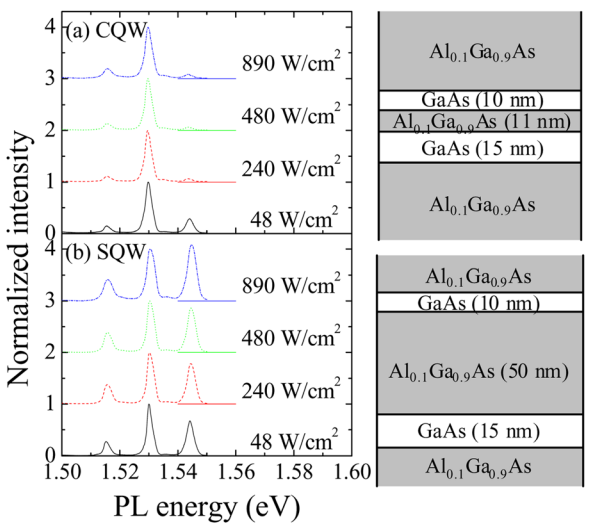


FIG. 1. (Color online) PL spectra from (a) CQW and (b) SQW. Solid (black), dashed (red), dotted (green), and dotted and dashed (blue) curves indicate spectra with excitation power densities of 48, 240, 480, and 890 W/cm$^2$, respectively. Each spectrum is normalized by the peak intensity of the LC mode or LS emission. Schematic sample structures are depicted on the right-hand side of each spectrum.

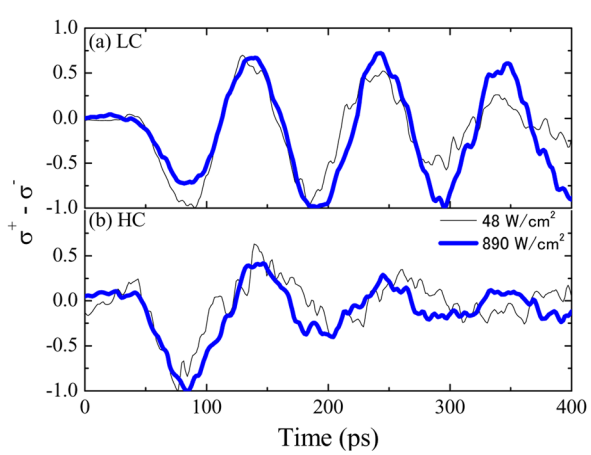


FIG. 2. (Color online) Time evolution of the PL intensity-difference $\sigma^+ - \sigma^-$ of (a) LC mode and (b) HC mode. Thin (black) and thick (blue) curves indicate excitation power densities of 48 and 890 W/cm$^2$, respectively. Each signal is normalized by the peak value.

Fig. 3. The peaks in the FT spectra correspond to a Larmor frequency of the spin precession. The Larmor frequency of the LC mode was same as that of the LS emission and was independent of the excitation power density as shown in Fig. 3(a). In Fig. 3(b), the Larmor frequency of the HC mode at a low excitation power was almost the same as that of the HS emission in Fig. 3(c). Although the Larmor frequency of the HS emission was independent of the excitation power density, that of the HC mode was shifted toward that of the LC mode as the excitation power density increased.

## III. THEORETICAL ANALYSIS

To discuss the dependence of the Larmor frequency on the excitation power density observed in our measurements, we take into account the Zeeman energy under an external magnetic field $\mathbf{B}_{ext} = (B_{ext}, 0, 0)$, where the $z$-axis is parallel to the direction of quantum confinement, and an effective magnetic field $\mathbf{B}_{eff}^{\beta}$ caused by an electron system $\beta$ in our theoretical calculations. The Hamiltonian used in the calculations for an electron system $\alpha$ is

$$\mathbf{H}^{\alpha} = \mu_B g_{\perp}^{\alpha} \mathbf{S} \cdot \left( \mathbf{B}_{ext} + \mathbf{B}_{eff}^{\beta} \right). \tag{1}$$

Here, $\mu_B$ is a Bohr magneton. When we calculated the electron spin state in the HC mode, we adopted this mode as the system $\alpha$ and the LC mode as the system $\beta$. In an opposite manner, the LC and HC modes were adopted as the systems $\alpha$ and $\beta$, respectively, for calculating the electron in the LC mode. $g_{\perp}^{\alpha}$ is a transverse $g$-factor of the electron in the system $\alpha$. The value of the transverse g-factors for the HC and LC modes used in this calculation are $g_{\perp}^{HC} = -0.26$ and $g_{\perp}^{LC} = -0.34$, respectively. $\mathbf{S} = (1/2)\boldsymbol{\sigma}$ is an electron-spin operator given by a Pauli matrix, $\boldsymbol{\sigma}$. $\mathbf{B}_{eff}^{\beta}$ is the effective magnetic field caused by the electron spin–spin interaction in system $\beta$. In this calculation, we assumed that the direction of the effective magnetic field is determined by an expected value of the electron spin averaged over the electron system $\beta$, $\langle \mathbf{S}^{\beta} \rangle = \mathrm{Tr}[\boldsymbol{\rho}^{\beta} \mathbf{S}]$. Here, $\boldsymbol{\rho}^{\beta}$ is a density matrix for the electron system $\beta$. The magnitude of the effective magnetic field is considered to be proportional to a two-dimensional (2D) density of the electrons in the system $\beta$, $N^{\beta}$. The ratio of the 2D density of the electrons in the HC and LC modes is assumed to be $N^{HC} : N^{LC} = 1 : 6$, considering the experimental intensity ratio averaged over the time domain.

The temporal evolution of density matrices for the electron system $\alpha$, $\boldsymbol{\rho}^{\alpha}$, was calculated by

$$\frac{d}{dt}\boldsymbol{\rho}^{\alpha} = \frac{1}{i\hbar}[\mathbf{H}^{\alpha}, \boldsymbol{\rho}^{\alpha}] + \boldsymbol{\Gamma}. \tag{2}$$

Here, $\hbar$ is Planck's constant and $\boldsymbol{\Gamma}$ is a spin coherence and a carrier relaxation term. The spin relaxation rate is assumed to be proportional to the difference in the electron density $n_{\uparrow}^{\alpha} - n_{\downarrow}^{\alpha}$ with a spin lifetime of $\tau_s^{\alpha}$. The carrier relaxation rate is proportional to the electron densities $n_{\uparrow}^{\alpha}$ and $n_{\downarrow}^{\alpha}$ with a carrier lifetime of $\tau^{\alpha}$. The spin lifetime $\tau_s^{\alpha}$, which is 500 ps for both the HC and LC modes, was obtained from our experimental results. The carrier lifetime $\tau^{\alpha}$ for the HC and LC modes used in this calculation were 240 and 470 ps, respectively, based on our experimental results. Substituting the Hamiltonian of Eq. (1) into the motion equation of Eq. (2), three differential equations are obtained. Note that to calculate the electron density in the system $\alpha$, the anti-diagonal elements in the system $\beta$ are necessary. Therefore, we solved six coupled equations based on Eqs. (1) and (2).

For comparison with experimental results, we performed a Fourier transformation (FT) of the calculated time traces. Figure 4 shows calculated FT spectra for the electron in Fig. 4(a) the HC mode and Fig. 4(b) the LC mode under an external magnetic field $\mathbf{B}_{ext}$ of 2 T. The ratios of the effective magnetic field to the external magnetic field $R^{\alpha} = |B_{eff}^{\beta}|/|B_{ext}|$ used in this calculation were 0.068 (solid line), 0.34 (dashed line), 0.68 (dotted line), and 1.26 (dotted and dashed line) for the HC mode and

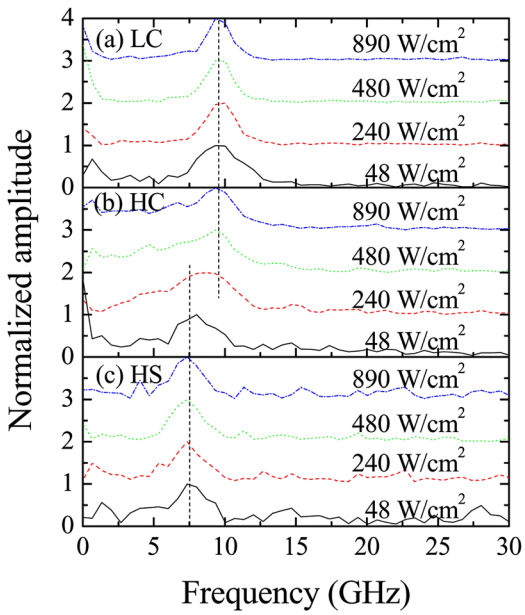


FIG. 3. (Color online). FT spectra of the measured spin precession signals of (a) LC mode, (b) HC mode, and (c) HS emission. Solid (black), dashed (red), dotted (green), and dotted + dashed (blue) curves indicate excitation power densities of 48, 240, 480, and 890 W/cm$^2$, respectively. Each spectrum is normalized by the peak intensity.

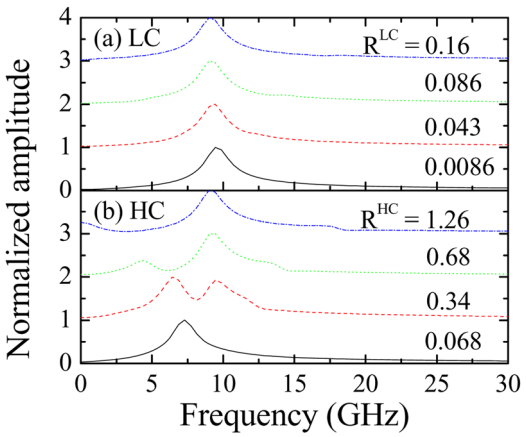


FIG. 4. (Color online). Calculated FT spectra of (a) LC and (b) HC mode emissions. The ratio of the effective to the external magnetic field, $R^{\alpha}$, is indicated near each spectrum. Each spectrum is normalized by the peak intensity.

0.0086 (solid line), 0.043 (dashed line), 0.086 (dotted line), and 0.16 (dotted and dashed line) for the LC mode. We assumed that the magnitude of the effective magnetic field was proportional to the 2D density of the electrons in the system $\beta$, $N^{\beta}$. We increased the total 2D density of excited electrons $N$ in correspondence with the experimental excitation power density ratios of 48 W/cm$^2$:240 W/cm$^2$:480 W/cm$^2$:890 W/cm$^2$ = 1:5:10:19. The peak frequency of the FT spectra (Larmor frequency) is independent on the effective magnetic field for the LC mode as shown in Fig. 4(a). The Larmor frequency in the HC mode shifted from that in the HS emission to the LC mode as the effective magnetic field increased, as shown in Fig. 4(b). These dependencies of the Larmor frequency on the effective magnetic field, which correspond to those on the excitation power density, were similar to our experimental results.

## IV. DISCUSSION

Here we consider that an electron spin-spin interaction between the electron systems $\alpha$ and $\beta$ is the physical origin of the effective magnetic field, and discuss the order of the contribution of the spin-spin interaction. We assumed that the main contributor to the spin–spin interaction is the exchange interaction and estimated the magnitude of this interaction in our experiments.

Under a Hartree-Fock approximation, the average exchange interaction energy for three-dimensional (3D) GaAs bulk[15] using an electron 3D density of $n^{\beta}$ in the system $\beta$ is

$$\varepsilon_{ex}\left(n^{\beta}\right) = -\frac{3}{4\pi A}\frac{e^2}{4\pi\varepsilon}\Big/\left(\frac{3}{4\pi n^{\beta}}\right)^{1/3}. \tag{3}$$

Here, $e$ is an electron charge, $\varepsilon$ is a permittivity of GaAs, and $A = (4/9\pi)^{1/3}$.

In an estimation of the exchange energy for CQW experiments, the exchange energy of the electron in the system $\alpha$ affected by the system $\beta$ was calculated using the exchange interaction energy of the system $\beta$, $\varepsilon_{ex}\left(n^{\beta}\right)$, and the overlap rate of a probability distribution of the electron in each system $P^{\alpha}$:

$$E_{ex}^{\alpha} = \varepsilon_{ex}\left(n^{\beta}\right)P^{\alpha}, \tag{4a}$$

$$P^{\alpha} = \frac{\int |\varphi^{\alpha}(x)|^2 |\varphi^{\beta}(x)|^2 dx}{\int |\varphi^{\beta}(x)|^2 |\varphi^{\beta}(x)|^2 dx}. \tag{4b}$$

$\varphi^{\alpha}(x)$ and $\varphi^{\beta}(x)$ are wave functions in the CQW for each system, which is calculated by one-band approximation. When distributions of electrons of system $\alpha$ and $\beta$ are completely overlapped, $P^{\alpha} = 1$. In this case, the exchange energy of an electron in the system $\alpha$ correspond to the average exchange interaction energy in the system $\beta$ $\left[\text{i.e., } E_{ex}^{\alpha} = \varepsilon_{ex}\left(n^{\beta}\right)\right]$. On the other hand, $P^{\alpha} = 0$ when they are completely different from each other. Thus, the exchange energy of an electron in the system $\alpha$ affected by the system $\beta$ becomes $E_{ex}^{\alpha} = 0$. In this calculation we roughly approximate that the $E_{ex}^{\alpha}$ is proportional to the $P^{\alpha}$ when distribution of the electrons in each system is partly overlapped as described in Eq. (4a). $P^{HC} \cong P^{LC} = 3 \times 10^{-3}$ is obtained from calculated $\varphi^{\alpha}(x)$ and $\varphi^{\beta}(x)$. The ratio of the electron 2D densities in the HC and LC modes are assumed to be $N^{HC} : N^{LC} = 1 : 6$, considering the PL intensity in our experiments. From the one-band approximation calculation, the distribution volume of electrons in the HC and the LC modes is proportional to the well width. Thus, the ratio of the electron 3D density for each mode is assumed to be $n^{HC} : n^{LC} = 1 : 4$.

In our experiments, the Larmor frequency starts to shift when the excitation power density is around 240 W/cm$^2$. This excitation power corresponds to the excited electron 3D density per one pulse of $n \approx 1 \times 10^{17}\text{cm}^{-3}$. Here, the repetition rate of the excitation laser (i.e., 80 MHz) is considered. The absorption length of GaAs is assumed to be 1 $\mu$m. Using the electron 3D density of $n \approx 1 \times 10^{17}\text{cm}^{-3}$, we calculated the ratio of the exchange energy to the Zeeman energy; $r^{HC} = 0.37$. The Zeeman energy of the electron in the HC mode under a magnetic field of 2 T is 30 $\mu$ eV. Thus, the calculated exchange energy of the HC mode $E_{ex}^{HC}$ when the Larmor frequency starts to shift is around 10 $\mu$ eV. The energy ratio $r^{HC}$ corresponds to the ratio of the magnetic fields $R^{HC} = |B_{eff}^{LC}|/|B_{ext}|$. In theoretical calculations using Eqs. (1) and (2), the Larmor frequency started to change when the ratio was $R^{HC} = 0.34$. Although the estimated exchange energy of the HC mode $E_{ex}^{HC}$ is obtained from the average exchange energy $\varepsilon_{ex}$ in 3D bulk GaAs, the order of the ratio obtained from Eq. (4), $r^{HC} = 0.37$, is very close to that obtained from Eqs. (1) and (2), $R^{HC} = 0.34$, at the excitation power at which the Larmor frequency starts to shift.

We now discuss the propriety of the assumptions used in present study. In the theoretical analysis on the spin-spin interaction, we assumed that the excited photocarriers relax to the HC and LC modes within a few ps and then moderately relax from the HC to the LC mode. It is known that the temperature of the excited carriers is cooled down to the lattice temperature within a few tens of ps. Any influence of the hot carriers on the measured Larmor frequency is considered small because the spin precession has been measured over a few hundreds of ps. Given that the measurements are performed at 4 K, phonons that may cause carrier scatterings are almost frozen.

Photoluminescence spectra are known to correctly reflect the energy distributions of electrons in the subbands because the effective mass of electrons is sufficiently smaller than that of holes. Even at the highest excitation density ($10^{11}\text{cm}^{-2}$) the PL width of the LC mode is kept almost the same as that at low excitation. The pileup of electrons in the LC mode (electron quasi-Fermi energy of 4 meV for the high excitation condition) is sufficiently small compared to the energy difference between the LC and HC modes (15 meV). Thus, the PL peaks of the HC mode are observed as distinct peaks, as shown in Fig. 1(a). If the pileup of electrons in the LC mode had seriously occurred at the high excitation condition, a broadening and shift of the peaks should have been observed in the Larmor frequency spectra of the LC mode because the g-factor value is energy-dependent. However, neither a broadening nor a shift is observed in the measured Larmor frequency spectra of the LC mode [Fig. 3(a)].

In the present theoretical analysis, we have considered only spin-dependent exchange energy (the real part of electron self-energy). Spin exchange (the imaginary part of the self-energy)

is another mechanism that may cause spin transfer between subbands via electron-electron scattering.[16] However, even if some spins are transferred from the LC to the HC mode through electron-electron scattering, the precession oscillation of the transferred spin is smoothed out because the scattering occurs randomly and the Larmor frequency of the LC mode is different from that of the HC mode. Hence, the effect of the electron-electron scattering on the precession frequency of the HC mode is likely to be small.

Finally, we emphasize that present experimental results are quantitatively explained by the spin-dependent exchange energy. A more precise analysis of the exchange energy and spin exchange via electron-electron inter-subband scattering in the CQW is expected. We hope that our experimental data will be helpful for such calculations in the future.

## V. CONCLUSIONS

We have observed the spin–spin interaction effect in spin precession through polarization- and time-resolved PL measurements. The electron spin-spin interaction effect was observed when the ratio of the effective to the external magnetic field was around $R^{HC} = 0.34$. Nearly the same value was obtained from an estimation considering the exchange energy. Remarkably, the exchange interaction effect appeared in the Larmor frequency of the electron in a coupled quantum well. This is an indication that despite the barrier layer, substantial overlap between electronic wavefunctions predominantly localized in the neighboring wells causes exchange interaction responsible for our observations. Fundamental physics of spin interactions in CQW structures revealed by this study can contribute to the development of quantum information technologies.

[1]B. E. Kane, Nature (London) **393**, 133 (1998).
[2]D. Loss and D. P. DiVincenzo, Phys. Rev. A **57**, 120 (1998).
[3]G. Burkard, D. Loss, and D. P. DiVincenzo, Phys. Rev. B **59**, 2070 (1999).
[4]A. Imamoglu, D. D. Awschalom, G. Burkard, D. P. DiVincenzo, D. Loss, M. Sherwin, and A. Small, Phys. Rev. Lett. **83**, 4204 (1999).
[5]T. D. Ladd, J. R. Goldman, F. Yamaguchi, Y. Yamamoto, E. Abe, and K. M. Itoh, Phys. Rev. Lett. **89**, 017901 (2002).
[6]S. M. Clark, Kai-Mei C. Fu, T. D. Ladd, and Y. Yamamoto, Phys. Rev. Lett. **99**, 040501 (2007).
[7]R. Vrijen and E. Yablonovitch, Physica E **10**, 569 (2001).
[8]H. Kosaka, H. Shigyou, Y. Mitsumori, Y. Rikitake, H. Imamura, T. Kutsuwa, K. Arai, and K. Edamatsu, Phys. Rev. Lett. **100**, 096602 (2008).
[9]A. Tackeuchi, T. Kuroda, Y. Nakata, M. Murayama, T. Kitamura, and N. Yokoyama, Jpn. J. Appl. Phys. **42**, 4278 (2003).
[10]K. Morita, H. Sanada, S. Matsuzaka, Y. Ohno, and H. Ohno, Appl. Phys. Lett. **94**, 162104 (2009).
[11]A. P. Heberle, W. W. Ruhle, and K. Ploog, Phys. Rev. Lett. **72**, 3887 (1994).
[12]M. Oestreich and W. W. Ruhle, Phys. Rev. Lett. **74**, 2315 (1995).
[13]I. Y. Gerlovin, Y. K. Dolgikh, S. A. Eliseev, V. V. Ovsyankin, Y. P. Efimov, I. V. Ignatiev, V. V. Petrov, S. Y. Verbin, and Y. Masumoto, Phys. Rev. B **69**, 035329 (2004).
[14]T. Ito, W. Shichi, S. Morisada, M. Ichida, H. Gotoh, H. Kamada, and H. Ando, Phys. Status Solidi C **3**, 3496 (2006).
[15]C. Kittel, *Quantum Theory of Solids* (Wiley, New York, 1987).
[16]P. Harrison, *Quantum Wells, Wires, and Dots,* 8.9 Carrier-Carrier Scattering (Wiley, New York, 2000); and related papers therein.